Biochimica et Biophysica Acta 1822 (2012) 1284–1292

Contents lists available at SciVerse ScienceDirect

Biochimica et Biophysica Acta

journal homepage: www.elsevier.com/locate/bbadis

Mutations at the flavin binding site of ETF:QO yield a MADD-like severe phenotype in *Drosophila*

Ema Alves [a,b], Bárbara J. Henriques [a], João V. Rodrigues [a], Pedro Prudêncio [b], Hugo Rocha [c], Laura Vilarinho [c], Rui G. Martinho [b,d,*], Cláudio M. Gomes [a,**]

[a] *Instituto Tecnologia Química e Biológica, Universidade Nova de Lisboa, Oeiras, Portugal*
[b] *Instituto Gulbenkian de Ciência, Oeiras, Portugal*
[c] *Unidade de Rastreio Neonatal, Instituto Nacional de Saúde, Porto, Portugal*
[d] *Dept. Ciências Biomédicas e Medicina, Universidade do Algarve, Portugal*

ARTICLE INFO

Article history:
Received 18 July 2011
Received in revised form 3 May 2012
Accepted 4 May 2012
Available online 9 May 2012

Keywords:
Flavoprotein
Drosophila
Multiple acyl-CoA dehydrogenase deficiency (MADD)
Inherited metabolic defect
Rossmann fold
Acylcarnitines

ABSTRACT

Following a screening on EMS-induced *Drosophila* mutants defective for formation and morphogenesis of epithelial cells, we have identified three lethal mutants defective for the production of embryonic cuticle. The mutants are allelic to the *CG12140* gene, the fly homologue of electron transfer flavoprotein:ubiquinone oxidoreductase (ETF:QO). In humans, inherited defects in this inner membrane protein account for multiple acyl-CoA dehydrogenase deficiency (MADD), a metabolic disease of β-oxidation, with a broad range of clinical phenotypes, varying from embryonic lethal to mild forms. The three mutant alleles carried distinct missense mutations in ETF:QO (G65E, A68V and S104F) and maternal mutant embryos for ETF:QO showed lethal morphogenetic defects and a significant induction of apoptosis following germ-band elongation. This phenotype is accompanied by an embryonic accumulation of short- and medium-chain acylcarnitines (C4, C8 and C12) as well as long-chain acylcarnitines (C14 and C16:1), whose elevation is also found in severe MADD forms in humans under intense metabolic decompensation. In agreement the ETF:QO activity in the mutant embryos is markedly decreased in relation to wild type activity. Amino acid sequence analysis and structural mapping into a molecular model of ETF:QO show that all mutations map at FAD interacting residues, two of which at the nucleotide-binding Rossmann fold. This structural domain is composed by a β-strand connected by a short loop to an α-helix, and its perturbation results in impaired cofactor association via structural destabilisation and consequently enzymatic inactivation. This work thus pinpoints the molecular origins of a severe MADD-like phenotype in the fruit fly and establishes the proof of concept concerning the suitability of this organism as a potential model organism for MADD.

1. Introduction

Multiple acyl-CoA dehydrogenase deficiency (MADD, OMIM: 231680), also known as glutaric aciduria type II, is an inherited disorder of the mitochondrial fatty acid β-oxidation (FAO) which results from defects in either electron transfer flavoprotein (ETF) or in electron transfer flavoprotein:ubiquinone oxidoreductase (ETF:QO). These two proteins constitute a metabolic hub through which electrons shuttled by at least 11 acyl-CoA dehydrogenases (ACDHs), resulting from fatty acid oxidation, amino acid and choline catabolism [1], are transferred to the mitochondrial respiratory chain via the quinone pool. ETF is a dimer of 30 kDa (ETFα) and 28 kDa (ETFβ) subunits held by a structural AMP and containing a FAD which oxidises the different ACDHs shuttling electrons to ETF:QO, its redox partner. ETF:QO is a 64 kDa monomer which binds to the inner mitochondrial membrane possibly via an amphipatic helix, and it contains different cofactors ([4Fe–4S], FAD, ubiquinone) organised in distinct structural domains. Genetic lesions in any of the genes encoding for these proteins, frequently point mutations, yield rather distinct clinical phenotypes. These range from extremely severe forms resulting in death at the embryonic (type I) or neonatal stage (type II), to mild forms (type III) which can be controlled through diet and in some cases riboflavin [2], carnitine and CoQ10 supplementation. Nevertheless, even these 'mild' cases are frequently life-threatening,

Abbreviations: FAO, fatty acid β-oxidation; MADD, multiple acyl-CoA dehydrogenase deficiency; ETF:QO, electron transfer flavoprotein:ubiquinone oxidoreductase; ETF, electron transfer flavoprotein; CoA, coenzyme A; MCAD, medium chain acyl-CoA dehydrogenase; SCAD, short chain acyl-CoA dehydrogenase; EMS, ethyl methanesulfonate; FAD, flavin adenine dinucleotide

* Correspondence to: R.G. Martinho, IGC, R. Quinta Grande 6, 2780-156 Oeiras, Portugal. Tel.: +351 214407906; fax: +351 214407970.
** Correspondence to: C.M. Gomes, ITQB/UNL, Av. República 127, 2780-756 Oeiras, Portugal. Tel.: +351 214469332; fax: + 351 214411277.
E-mail addresses: rmartinho@igc.gulbenkian.pt (R.G. Martinho), gomes@itqb.unl.pt (C.M. Gomes).
URL: http://www.itqb.unl.pt/pbfs (C.M. Gomes).

0925-4439/$ – see front matter © 2012 Elsevier B.V. All rights reserved.
doi:10.1016/j.bbadis.2012.05.003

for example in children as a result of metabolic decompensation during fever and sugar depletion.

The functional failure in ETF and ETF:QO variants carrying missense mutations has multiple origins, from defects in protein biogenesis, folding and stability, to catalytic impairment due to a perturbation of the cofactors. Among these, FAD plays a pivotal role, not only in ETF [3,4] and ETF:QO, but also in all acyl-CoA dehydrogenases which also harbour this organic cofactor [5]. In fact, the flavin moiety is determinant for protein structure and function: catalytically, it is very versatile as its oxidation–reduction properties can be fine-tuned through interactions with the polypeptide chain at the binding pockets [6,7], and the many structures available also show the important structural role it plays in the protein three-dimensional organisation [8–13]. This cross-talk is clearly illustrated in the Rossmann fold, a nucleotide binding structural domain also present in ETF:QO, which comprises a β-strand connected by a short loop to an α-helix, and includes an expanded sequence motif ($V/IxGx_{1-2}GxxGxxxG/A$) that affords both FAD binding and stabilisation of the secondary structure elements involved [14]. Small changes in the FAD interacting residues may change the redox potential of the flavin, its affinity towards the protein, or ultimately disrupt binding, with consequent enzymatic inactivation and structural disruption. Moreover, the relevance of flavins as cofactors also results from the fact that they are able to carry out both one and two electron transfer reactions [2].

In spite of a growing understanding of the biochemical details of defective processes in β-oxidation, as well as an increasing expansion of the genotypic and phenotypic characteristics of patients suffering from MADD, the fact is that cellular studies have been mostly limited to patient fibroblasts. However, recent studies have opened the perspective of implementing organism models for MADD by addressing the effects of defects in ETF:QO in zebrafish and in the nematode *Caenorhabditis elegans* [15,16]. These have been the cases of the study on the zebrafish mutant *xav* which corresponds to a non-sense mutation that results in an inactivating truncation of ETF:QO [15], and in the nematode, two mutant alleles of *let-721* which correspond to deleterious point mutations in ETF:QO [16]. These studies exemplify how model organisms can contribute to a broader biological understanding of processes affected in MADD—for example the zebrafish study elicited that neurogenesis is affected through the PPARG–ERK pathway and the nematode work puts in evidence that ETF:QO is expressed under complex transcriptional control.

In this work we report the genotypic, phenotypic and biochemical characteristics of a severe MADD-like phenotype in the fruit fly *Drosophila melanogaster*, establishing the proof of principle concerning the suitability of this organism as a potential model not only for MADD but also for inherited fatty acid disorders in general. Our focus on this study has been to correlate developmental defects of *Drosophila* mutants with specific alterations at the level of protein structure and stability. We have established that three independent mutant alleles, corresponding to three distinct point mutations in ETF:QO, are lethal as a result of a specific knock-down of FAD binding by direct disruption of the cofactor binding motif within the nucleotide binding Rossmann fold. This study thus provides a direct molecular rationale for the effect of specific mutations at the cellular and structural levels, and offers a platform to test in *Drosophila* a range of MADD-mutations yielding diverse clinical phenotypes, from severe to milder forms of the disease.

2. Materials and methods

2.1. Fly work

All *ETF:QO* alleles were isolated from a previously reported maternal screen [17]. All flies were raised at 25 °C using standard techniques. Riboflavin supplementation of the medium was also tested from 0.2 to 5 mM. To generate *ETF:QO* mutant clones (negative for nuclear GFP label; nGFP*minus*), females y, w, hsFLP; FRT42B nGFP/CyO hshid were crossed with males w; FRT42B, *ETF:QO*/CyO. The offspring was heat-shocked two times for 1 h at 37 °C during second and third *instar* larvae. To generate homozygous clones of *ETF:QO* in wing imaginal discs, female y, w, hsFLP; FRT42B nGFP/CyO hshid flies were crossed with w; FRT42B, *ETF:QO*/CyO males. The offspring was heat shocked for 1 h at 37 °C, 48 h after a 24-hour egg collection, corresponding to second *instar* larvae. Wing discs were dissected from crawling third *instar* larvae. Maternal mutant embryos for *ETF:QO* were obtained using the FLP/FRT*ovoD* system [18]. w; FRT42B *ETF:QO*/CyO virgins were crossed to y, w, hsFLP; FRT42B *ovoD*/CyO hshid males at 25 °C and the progeny was heat-shocked two times at 37 °C for 1 h during second and third *instar*.

2.2. Mapping and cloning of ETF:QO alleles

Complementation Group 1 mutant alleles were mapped using the Bloomington 2R deficiency kit to chromosome region 46C. By a candidate gene approach we concluded that all three different alleles of Group 1 (A56-12, B42-1 and B43-36) were most likely mutant alleles of *ETF:QO* as they failed to complement a lethal P-element (*w[1118]; PBac{w[+mC]=WH}CG12140[f05640]*) associated with the *ETF:QO* gene *locus*. Molecular characterisation of the isolated *ETF:QO* alleles identified different point mutations within the coding region of this gene. All mutations were independently sequenced three times from different PCR reactions and we used a mutant allele isolated in the same screen but from a different complementation group to identify single-nucleotide polymorphisms present in the original mutagenised stock.

2.3. Immunostainings

Third *instar* wing imaginal disc fixation and staining were performed using standard procedures [19]. For maternal phenotypic analysis, embryos were fixed and stained using standard procedures [17]. The oogenesis phenotypic analysis was performed with tissue dissected from 2 or 3 days old females where mutant clones were induced by heat-shock at second *instar* larvae stages, and fixed in phosphate buffered saline (PBS) with 4% formaldehyde for 20 min. Primary antibodies used were anti-Armadillo N2 7A1 mouse at 1:20 (Developmental Studies Hybridoma Bank (DSHB)), anti-Cleaved Caspase-3 rabbit at 1:500 (Cell Signaling, 9661S), anti-Neurotactin mouse clone BP106 at 1:133 (DSHB) and anti-pTyr mouse at 1:1000 (Cell Signaling, 9411). Secondary antibodies were Cy3- and Cy5-conjugated at 1:1000 (Jackson ImmunoResearch Laboratories, West Grove, PA). For F-Actin staining, Phaloidin-Rhodamine was used at 1:200 (Sigma) (stock concentration 1 $mg.ml^{-1}$) with 5 min incubation. Ovaries and embryos were mounted in fluorescent mounting medium (DakoCytomation, Inc.) and wing discs were mounted in Vectashield (Vector Laboratories). Samples were visualised with a Leica SP5 confocal microscope.

2.4. Acylcarnitine analysis

For each assay, approximately 20 mg of biological samples was used. The thawed embryos, which had been harvested 0–6 h after egg laying and stored in 20% Glycerol at −80 °C, were centrifuged at 12,000×*g* for 10 min to remove glycerol. Embryos were then resuspended in 200 µl of sucrose buffer (200 mM sucrose, 10 mM MOPS pH 7.2, 0.1 mM EDTA) and centrifuged again. Sucrose buffer was removed and the embryos were washed two more times before being homogenised with a pestle in sucrose buffer containing 0.5 mM of phenylmethylsulphonylfluoride (PMSF) (Roth). The solutions were sonicated during 30 s at 10% intensity 2 times, with an interval of 1 min, before being submitted to a speed vacuum in order to decrease the volume to approximately 50 µl. The embryo proteins were quantified by the Bradford method, and the same amount of protein was applied in the Whatman 903® filter paper and dried overnight away from light. Acylcarnitine analysis by MS/MS spectrometry was carried out as

previously described [20], with slight modifications. Embryo extracts contained a number of unknown substances that overlap with some of the acylcarnitine standards used in the MS/MS analysis, and therefore, unlike in blood samples for which the protocol used is optimised, it is not possible to carry out the measurements of the routine broad range of acylcarnitines. Thus, the results obtained refer exclusively to the metabolites which had no interference and could be accurately determined: free carnitine (C0) and the carnitine derivatives of acetyl-CoA (C2), butyryl (C4), octanoyl (C8), dodecanoyl (C12:0), tetradecanoyl (C14:0) and hexadecenoyl (C16:1)—see Results and discussion and Supplementary Table S1.

2.5. Western blot analysis

Embryos were resuspended in 200 µl of 50 mM Tris pH 7.5, with 3% SDS, 0.1 mM DTT, 1 mM EDTA, and 1 mM PMSF, and were lysed with the help of plastic pestles against the walls of a 1.5 ml microtube. The samples were centrifuged for 10 min at 20,000×*g*, and the pellet was resuspended again with the plastic pestle. The suspension was incubated at 37 °C for 30 min and, centrifuged at 20,000×*g* for 10 min. Protein concentration was determined by a modified Biuret method [21]. Samples (50 µg of total protein) were separated using SDS-PAGE followed by western blotting analysis. Equal gel loading and blotting efficiency was assessed by the total protein staining of the PVDF membrane with Coomassie [22]. An ETF:QO polyclonal antibody raised in rabbits against two synthetic human ETF:QO peptides (p.48I_62M and p.485T_499A) was used to identify ETF:QO proteins [23] and visualised with a peroxidase conjugated secondary antibody reaction with Amersham ECL Prime solution (GE Healthcare).

2.6. ETF:QO activity

Thawed embryos were resuspended in 50 mM Tris–HCl pH 7.5, 1 mM DTT and 0.5 mM PMSF, and were lysed with the help of a plastic pestle against the walls of a 1.5 ml microtube. The suspension was centrifuged at 5000×*g*, 10 min, and a plastic pestle was used again to disrupt unbroken cells. The samples were sonicated four times at 20% amplitude with a 0.5 second pulse during 10 s. The membrane fraction was obtained by ultracentrifugation at 100,000×*g* for 1 h. The membranes were resuspended in 50 mM Tris–HCl pH 7.5 and dodecylmaldoside was added to a final concentration of 1%. After 1 h incubation at 4 °C, the samples were centrifuged at 10,000×*g*, and the supernatant was stored. The protein concentration was determined by the modified Biuret method [21].

The activity of ETF:QO was measured by the disproportionation assay as described in [24], with modifications. Experiments were performed using 1 cm path length quartz ultra-micro cell (Hellma) with 5×3 mm aperture, allowing the monitoring of low volume reactions (60 µl). The reaction mixture contained 50 mM Tris–HCl pH 7.5, 10 µM ETF, 6 units of catalase, and 1.8 unit glucose oxidase. The cuvette was sealed with a rubber stopper and degassed by 10 repetitions of vacuum/argon cycles. Glucose was added to a concentration of 30 mM and the solution was incubated for 10 min under an argon purge. ETF was reduced quantitatively to the semiquinone form with sodium dithionite, and the formation of the characteristic semiquinone spectrum was followed spectrophotometrically. The reaction was initiated by the addition of the membrane fractions from *Drosophila* embryos made anaerobic by repeated vacuum/argon cycles. The disproportionation of ETF was followed spectrophotometrically in dual wavelength mode at 374 nm and 437 nm. The initial velocities were determined from the traces resulting from the subtraction of the absorbances at 374 nm and 437 nm, and the extinction coefficient of 9000 $M^{-1}.cm^{-1}$ was used [25]. At least three replicate measurements were performed for each variant.

2.7. Sequence analysis and molecular model

The sequence of *Drosophila* ETF:QO was retrieved from the NCBI databank (P55931), together with those of its human (545621) and porcine (24652256) homologues. Multiple sequence alignment, sequence identity and similarity calculations, and motif analysis were carried out using Genedoc [26]. The crystallographic structure of porcine ETF:QO (PDB: 2gmh) was used to produce a structural model of the fly ETF:QO by homology modelling (Swiss-Model). The two proteins share a very high amino acid sequence identity (78%) thus making the porcine enzyme an excellent structural template. The porcine ETF:QO was used to carry out the analysis of the molecular interactions, cofactor contacts and topological features. These analyses, together with the prediction of the conformation of the side chains of the mutant residues were carried out using the WhatIF web server and the PDBsum database [27]. Structures were inspected using PyMOL (DeLano Scientific).

2.8. Cloning, expression and purification of Drosophila ETF

Drosophila ETFA cDNA cloned into pBlueScript SK vector was obtained from the Berkeley *Drosophila* Genome Project. *Drosophila ETFB* cDNA directionally cloned into the 5′EcoRI site and the 3′ XhoI site of pOT2 vector was obtained from Berkeley *Drosophila* Genome Project. The amplified sequences of *ETFA* and *ETFB* were assembled by means of various cloning and subcloning steps and introduced between the NcoI and AflII sites, and NdeI and AvrII sites, respectively, of the pETDuet-1 vector. Both target genes are preceded by a T7 promotor/*lac* operator and a ribosome binding site. *Escherichia coli* BL21 cells transformed with the drosophila ETF plasmid were grown at 30 °C in LB (Luria–Bertani) medium, supplemented with 100 $\mu g.ml^{-1}$ ampicillin, in a shaking incubator until OD_{532} of 0.5–0.8 was reached. Cells were then induced with 1 mM isopropyl-β-D-thiogalactopyranoside (IPTG) for 4 h, and after were harvested by centrifugation.

Cells were resuspended in 10 mM Hepes pH 7.8, 10% ethylene glycol and 0.5 mM PMSF (buffer A), in the presence of 0.1 $mg.ml^{-1}$ FAD (Sigma) and DNase (Applichem), and disrupted in a French press. The soluble extract was applied into a 20 ml Q-Sepharose fast flow (Amersham Biosciences) column equilibrated in buffer A. The column was washed with 5 column volumes of buffer A, and bound proteins were eluted by a linear gradient ranging from 0 to 1 M NaCl, in buffer A. ETF eluted as a pure protein at ~200 mM salt, as shown by SDS/PAGE. Protein concentration was determined using the Bradford assay, and flavin content was determined using the molar extinction coefficient $\varepsilon_{436\ nm} = 13{,}400\ M^{-1}.cm^{-1}$ reported for FAD bound to ETF [28]. The enzymatic activity of the purified protein was measured monitoring DCPIP reduction, in a coupled assay in which recombinant human MCAD and octanoyl-CoA were used, as described in [29]. One unit of catalytic activity is defined as nmol of DCPIP reduced per minute, in the conditions used in the assay. All specific activities reported are based on total flavin content. Far-UV circular dichroism, recorded on a Jasco J-715 spectropolarimeter with peltier temperature control, was used to analyse the protein fold and secondary structure. Thermal unfolding with a linear temperature increase was followed using circular dichroism (ellipticity variation at 222 nm), with a heating rate of 1 $°C.min^{-1}$ and temperature increased from 30 to 90 °C. A quartz polarised 1 mm path length cuvette (Hellma) was used, and protein concentration was 0.1 $mg.ml^{-1}$. Data were analysed according to a two-state model, and fits to the transition curves were made using Origin. The purified protein was fast-frozen using liquid nitrogen and stored at −80 °C.

2.9. Cloning and expression of Drosophila ETF:QO

Drosophila ETF:QO synthetic gene was cloned into pGS-21a vector between NdeI and HindIII cloning sites (GenScript, Inc). The *ETF:QO* gene is preceded by a T7 promotor/*lac* operator, and has a 6xHis-tag sequence in the N-terminus. ETF:QO-Ala68Val was also designed in

the same vector. Briefly, different conditions for cell growth including different *E. coli* cell types (BL21, JM109, C43, and Rosetta) and different temperatures (25 °C, 30 °C and 37 °C) were tested. Also, different growth media were used for each cell type: LB (10 g Bacto Tryptone, 5 g Bacto Yeast extract and 10 g NaCl per litre), dYT medium (16 g Bacto Tryptone, 10 g Bacto Yeast extract and 5 g NaCl per litre) and rich medium for auto induction [30]. All growth media were supplemented with 100 $\mu g.ml^{-1}$ ampicillin, and protein expression was induced with 100 μM–500 μM IPTG. Cells were harvested by centrifugation, and then resuspended in 20 mM Tris pH 8.0, 1 mM DTT and 0.5 mM PMSF, in the presence of DNase, and were disrupted in a French press. The extract was centrifuged at 10,000×*g* for 10 min, and the supernatant treated by ultracentrifugation at 100,000×*g* for 1 h. The membrane fraction was resuspended in 20 mM Tris pH 8.0 and dodecylmadoside was added up to 1% (w/v). The presence of ETF:QO was assayed by the quinone reduction method as described in [25].

3. Results and discussion

3.1. ETF:QO is maternally required for Drosophila embryogenesis

Previously we isolated close to 300 independent EMS-induced *Drosophila* mutant lines defective for formation and morphogenesis of epithelial cells [17]. From the 2R (right-arm of the second chromosome) secondary screen we isolated 47 lines out of the previously isolated 137 lines. These 47 mutant lines are defective for the production of embryonic cuticle (no cuticle or scraps of cuticle). Complementation studies of these mutants allowed the identification of nine 2R complementation groups. All three alleles of Complementation Group 1 were maternally lethal after induction of germ-line clones (data not shown). Similarly, transheterozygotes were also zygotic lethal (data not shown). Deficiency mapping and candidate gene approach suggested that Group 1 mutants were allelic to CG12140 gene (*ETF:QO* from here on), which encodes the *Drosophila* homologue of the electron transfer flavoprotein:ubiquinone oxidoreductase (ETF:QO), also referred in some literature as electron transfer flavoprotein dehydrogenase. The nucleotide changes accounting for the observed phenotypes corresponded to three distinct point mutations in the protein coding sequence: ETF:QO-p.Gly65Glu (G65E), ETF:QO-p.Ala68Val (A68V) and ETF:QO-p.Ser104Phe (S104F). As further discussed in a following section, the *ETF:QO* gene product comprises different structural domains, and all identified lesions map specifically within the FAD binding domain, indicating that this region is an extremely sensitive functional hotspot. In molecular genetics terms, although there are around 40 point mutations identified in MADD patients that affect the *ETF:QO* gene, none of them corresponds to the mutations here identified. Actually this is not surprising as the genetic diagnosis is mostly carried out in living patients after a positive result from metabolic profiling, meaning that these patients carry genetic lesions that correspond to milder forms of the disease (type III). The lethal phenotype mutations that we have observed in the *Drosophila* mutants would most likely result in embryonic or neonatal death, corresponding to one of the more severe forms of the disease (type I and II).

3.2. Maternal mutant embryos for ETF:QO display gross morphogenetic defects and induction of apoptosis

Once fertilised, early embryonic development of the maternal mutant embryos for *ETF:QO* was normal: without obvious mitotic defects during syncytial blastoderm (data not shown), with normal blastoderm cellularisation (Fig. 1E, F), and germ-band extension (Fig. 1G, H). Nevertheless, during the onset of germ-band retraction there were gross morphogenetic defects and a significant induction of apoptosis (Fig. 1I–L). These abnormalities were indistinguishable between the three isolated mutant alleles of *ETF:QO* (data not shown). These results are in apparent agreement with previous observations also reporting morphogenetic defects in zygotic mutants of *ETF* (*walrus*), which encode for electron transfer flavoprotein (ETF) that is the redox partner of ETF:QO [31]. Although the observed phenotypes in *ETF:QO* maternal mutant embryos are significantly more pleiotropic than the ones reported for zygotic mutants of *ETF*, this is most likely due to the strong maternal contribution of ETF (modENCODE Temporal Expression Profile) in these embryos (Fig. S1).

3.3. Clonal analysis of ETF:QO mutant alleles failed to identify developmental defects

Mutant clonal analysis of the isolated *ETF:QO* mutant alleles failed to identify somatic and germ-line defects during *Drosophila* development. Large somatic follicular clones mutant for *ETF:QO* correctly encapsulated the developing egg-chambers during stage 3 of the germarium (Fig. 1A, B), and the mutant follicular cells maintained a normal epithelial architecture during oogenesis (Fig. 1B, C). Likewise, egg-chamber development was normal when the germ-line was mutant for *ETF:QO*, with normal number of nurse cells (data not shown) and, normal determination, positioning and growth of the oocyte (Fig. 1B, D). Large mutant clones for *ETF:QO* were also normal in the highly proliferative larval wing disc epithelial cells (Fig. 1M–P), with normal tissue proliferation (Fig. 1M, N; the mutant clone that is negative for GFP has a similar size to the control two copies GFP twin-spot clone) and normal epithelial architecture (Fig. 1O, P; the junctional protein Armadillo is correctly localised in the epithelial cells adherents junctions).

It is surprising that clonal mutant analysis of *ETF:QO* during oogenesis and larval development failed to retrieve obvious developmental defects. We propose two alternative non-exclusive hypotheses to explain the absence of phenotypes: 1) *Drosophila* cells only require relatively low levels of ETF:QO expression/activity. Consistently, and since the *ETF:QO* mutant alleles probably contain a residual enzymatic activity, they only become rate limiting during mid-embryogenesis when expression of this gene is extremely low (modENCODE Temporal Expression Profile) (Fig. S1); 2) Wild-type cells are able to complement *ETF:QO* metabolic functions of nearby mutant cells, even in large mutant clones. Consistently, we only observe phenotypes in experimental conditions where the entire organism is mutant for *ETF:QO*.

Altogether, this suggests that *Drosophila* embryonic development is particularly sensitive to defects in the ETF/ETF:QO hub. In humans, severe genetic defects resulting in loss of the *ETF:QO* gene product account for one of the two most severe forms of MADD: either a neonatal-onset form with (type I) or without (type II) congenital and foetal anomalies. These are characterised by prominent congenital malformations that range from kidney malformations; facial dysmorphism with a high forehead, macrocephaly, low-set ears, hypertelorism and hypoplastic midface; muscular defects of the anterior abdominal wall; and brain anomalies like cerebral pachygyria and symmetric warty dysplasia of the cerebral cortex [32–35]. Riboflavin exerts a beneficial effect in some of the milder forms of MADD (type III) but we have not observed any rescue effect upon supplementation of the fly culture medium with this vitamin. Overall, the observed gross morphogenetic defects and apoptosis in the three independent *ETF:QO* alleles are highly suggestive of a complete dysfunction of the ETF:QO protein that leads to abnormal mitochondrial fatty acid oxidation.

3.4. Acylcarnitine levels in ETF:QO mutant embryos display a profile typical of MADD

The diagnosis of fatty acid β-oxidation disorders is made by analysing the levels of plasma acylcarnitines, which accumulate as a result of an enzymatic deficiency that blocks the metabolic pathway and causes the upstream build-up of fatty acyl-CoAs. In order to evaluate the level of dysfunction of mitochondrial fatty acid β-oxidation in our *Drosophila* mutant alleles, corresponding to the ETF:QO-G65E, ETF:QO-

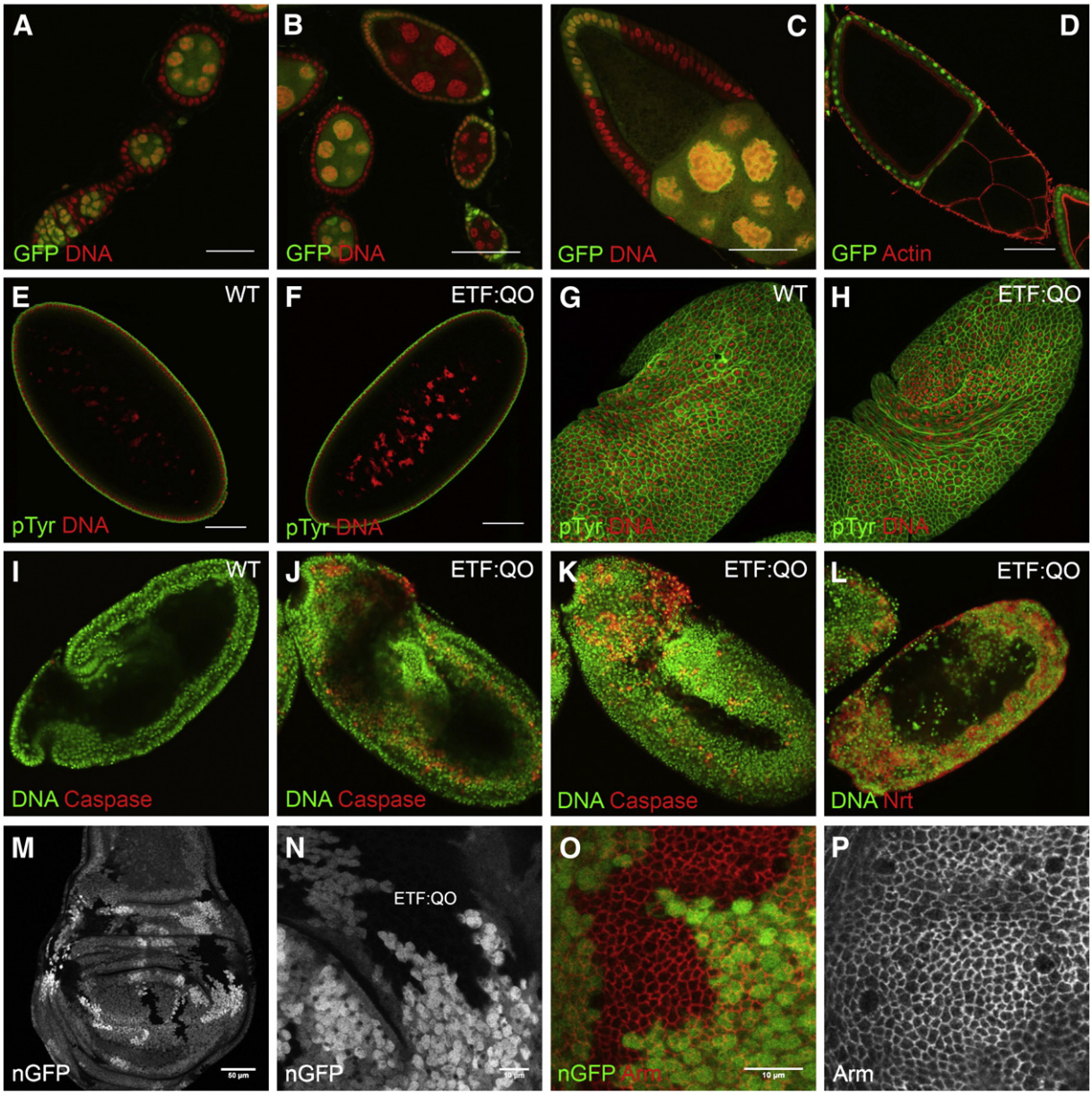

Fig. 1. *ETF:QO* maternal mutant embryos showed gross morphogenetic defects and induction of apoptosis during mid-embryogenesis. Mutant clones for *ETF:QO* (marked by the absence of nuclear GFP) (green (A–D)) showed no obvious defects during oogenesis, with a normal development of the somatic follicular epithelium (A–C) and of the germ-line (B, D). Maternal mutant embryos for *ETF:QO* showed a normal blastoderm cellularisation (E, F) and germ-band extension (G, H), yet subsequently, there were gross morphogenetic defects and a significant induction of apoptosis (I–L). Mutant clones of *ETF:QO* in wing imaginal discs did not affect cell proliferation (mutant clones marked by the absence of GFP had similar size to the control twin-spot clone marked by two copies GFP (M, detail in N) and epithelial architecture (O–P)). Wild type (E, G and I) and maternal mutant ETF:QO (F, H, J–L). Embryos were stained for DNA (red (E–H) and green (I–L)), activated cleaved caspase 3 (marker for apoptosis) (red (I–K)), pTyr (green (E–H)) and Neurotactin (Nrt; membrane marker) (red (L)). Ovaries were stained for DNA (red (A–C)) and Actin (red (D)). Wing imaginal discs were stained for Arm (red (O) and white (P)). The ETF:QO alleles used were A68V (A–C, F, M–P), G65E (D,H), and S104F (J–L). The scale bar equals 10 μm (N–O), 20 μm (A), 40 μm (B–C), 50 μm (D and M) and 60 μm (E–F).

A68V and ETF:QO-S104F mutations, we have measured the levels of free carnitine and acylcarnitine derivatives by tandem mass spectrometry (MS/MS) in embryos collected 0–6 h after egg laying (Fig. 2 and Table S1). The measurements were carried out on total extracts of mutant embryos using wild type embryos as reference. The results obtained clearly show that fatty acid β-oxidation (FAO) is impaired: the total amount of free carnitine (C0), which is used to shuttle fatty acids inside the mitochondria, and acetyl-CoA (C2), which is the end product of the β-oxidation pathway, are significantly diminished in the *ETF:QO* mutant alleles. The level of free carnitine in the mutant embryos (13–29 μM) is always lower than that of the wild type (39 μM), as well as the levels of produced acyl-CoA, which are rather decreased in the mutants (31–45 μM) in comparison to the levels in normal embryos (98 μM) (Table S1). Interestingly, the elevated levels of acylcarnitines in the mutant embryos are typical of MADD profiles: not only the short- and medium-chain acylcarnitines (C4, C8 and C12) are raised, but also the long-chain acylcarnitines (C14 and C16:1) whose elevation is restricted to severe MADD forms, or under metabolic decompensation (Fig. 2). However, the converse is not always true as MADD must involve functional deficiency within the ETF/ETF:QO hub.

3.5. Impaired ETF:QO activity in mutant embryos

To further characterise the effect of the mutations in ETF:QO we analysed protein levels in whole embryo extracts. Western blot analysis showed that polyclonal antibodies raised against human ETF:QO (see

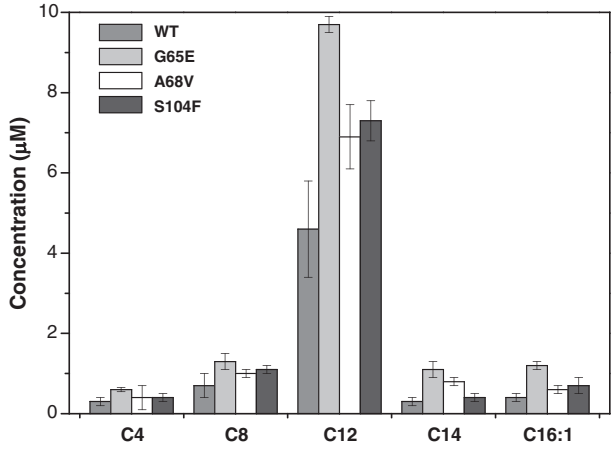

Fig. 2. *ETF:QO* maternal mutant embryos have raised acylcarnitine levels. The acylcarnitine levels were determined in maternal mutant embryos for the three isolated alleles (ETF:QO-G65E, ETF:QO-A68V and ETF:QO-S104F). The acylcarnitine concentrations represented were determined by MS/MS (n = 6). The following carnitine derivatives have been measured: butyryl (C4), octanoyl (C8), dodecanoyl (C12:0), tetradecanoyl (C14:0) and hexadecenoyl (C16:1). See Table S1 for concentrations and Materials and methods for details.

Materials and methods) cross-react with *Drosophila* ETF:QO protein as judged by the presence of a band with molecular mass matching the theoretical value of the mature protein (Fig. 3A). For the mutant embryos there is a clear decrease in ETF:QO protein levels which accounts for the observed MADD-like phenotype (Fig. 3A). A second band was also immune-detected at a lower molecular mass, most likely representing a degradation product of ETF:QO (Fig. 3A). Interestingly, this additional band is more intense in the mutants, suggesting that the mutated

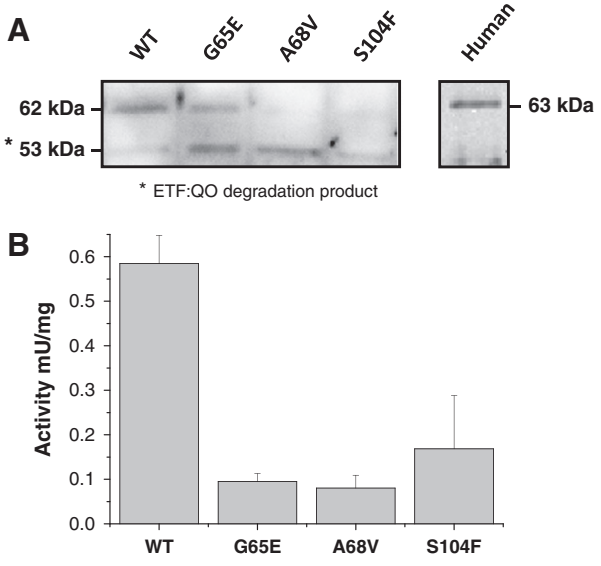

Fig. 3. ETF:QO protein levels are decreased in the maternal mutant embryos. Panel A: Whole cell lysates from *Drosophila* embryos were extracted in 3% SDS, separated using SDS/PAGE, and immunoblotted using a polyclonal antibody raised against human ETF:QO (see Materials and methods). Equal gel loading and blotting efficiency was assessed by the total protein staining of the PVDF membrane with Coomassie [22]. The western blot was repeated three times and a representative experiment is shown. Panel B: ETF:QO activity in isolated membranes from *Drosophila* embryos of different variants measured by the disproportionation assay. Solutions containing 10 μM ETF, 6 units of catalase, and 1.8 unit glucose oxidase were made anaerobic prior to the reduction of ETF to the semiquinone form using sodium dithionite. The reaction was initiated by the addition of anaerobic membrane fraction from embryos and the activity was calculated from the initial rates of disproportionation which was followed spectrophotometrically in dual wavelength mode at 374 nm and 437 nm (see Materials and methods). The bars show the average of at least three determinations and the error bars represent S.E.M.

proteins are more susceptible to degradation. In parallel to the decrease in protein levels, we found that the enzymatic activity measured in isolated membrane fraction of the embryos is also impaired in the mutants (Fig. 3B).

These data indicate that ETF:QO is not completely absent from the mutant *Drosophila* embryos, as a residual level of active protein is present. This does not exclude the possibility that mutations lead to the production of destabilised non-functional forms of the protein, as it is possible that the weak expression of ETF:QO is a result of a zygotic expression of wild-type protein (from a paternal wild-type chromosome) in the maternal mutant ETF:QO embryos.

In any case, the fact that the profiles of the three mutant alleles are similar to each other is in good agreement with the indistinguishable morphogenic phenotypes. Altogether, these results show that the three independent mutations in the *ETF:QO* mutant alleles dramatically decrease the levels of functional enzyme resulting in the accumulation of acylcarnitines as a consequence of a FAO blockage, thus severely affecting the energy and lipid metabolisms which lead to lethal morphogenic defects and embryo death.

In an attempt to characterise further this system we have carried out cloning and heterologous expression of *Drosophila* MADD proteins, ETF and ETF:QO. *Drosophila* ETF was successfully cloned, expressed and purified to homogeneity; the biochemical and structural characterisation of this protein showed that its properties are identical to those of its human homologue (Supplementary Fig. S2). However, despite all efforts (see Materials and methods) *Drosophila* ETF:QO was systematically expressed in the form of inactive inclusion bodies and no activity could be detected in membranes purified from *E. coli* cells overexpressing ETF:QO. In fact, the extreme difficulty of producing this protein has also been reported for human ETF:QO [36], and this likely results from the inability to correctly membrane-insert and assemble its multiple cofactors during overexpression. This negative result has prevented us to proceed with further biochemical studies on purified *Drosophila* MADD proteins.

3.6. Lethal mutations map at the FAD motif impairing cofactor binding

The fact that the three mutant *ETF:QO* alleles result in phenotypic and metabolic profiles identical to those found in severe MADD is strongly suggestive that the mutations are located in a functionally sensitive hotspot of the protein. In order to analyse the structural effects of the mutations on the protein, we have carried out a pair-wise comparison of the amino acid sequence of the *Drosophila* ETF:QO together with homologous sequences from man and pig (Fig. 4A and Fig. S3). *Drosophila* ETF:QO shares a high level of identity with these proteins (64% identity and 78% similarity), in particular in what concerns critical residues involved in: binding of the flavin (FAD) and [4Fe–4S] iron sulphur cluster (FeS) cofactors, interactions with ubiquinone (UQ), the catalytic pocket and putative membrane anchoring segments. The cofactors in the ETF:QO monomer are important structural elements, as they are essential to maintain the three dimensional organisation of the protein (Fig. 4B): perturbation of the FAD or FeS moieties results in protein disorganisation or ultimately in its unfolding or misassembly. A more detailed analysis of the identified mutations in the *Drosophila* mutant alleles shows that they all map at the FAD binding site, which is one of the crucial redox and catalytic cofactors of the protein (Fig. 4C). Indeed, two of the ETF:QO mutations (Gl65E, A68V) are directly located within the Rossmann fold, a nucleotide binding domain that begins with a β-strand connected by a short loop to an α-helix. For proteins that bind nucleotide cofactors, such as FAD, this fold comprises the expanded sequence motif V/IxGx$_{1-2}$GxxGxxxG/A. This sequence allows to: stabilise the β-strand and the α-helix, accommodate glycyl residues located in the connecting loop of cofactor pocket, and stabilise interactions between the two elements of secondary structure [14]. Therefore, this region is particularly sensitive to amino acid changes as the specific

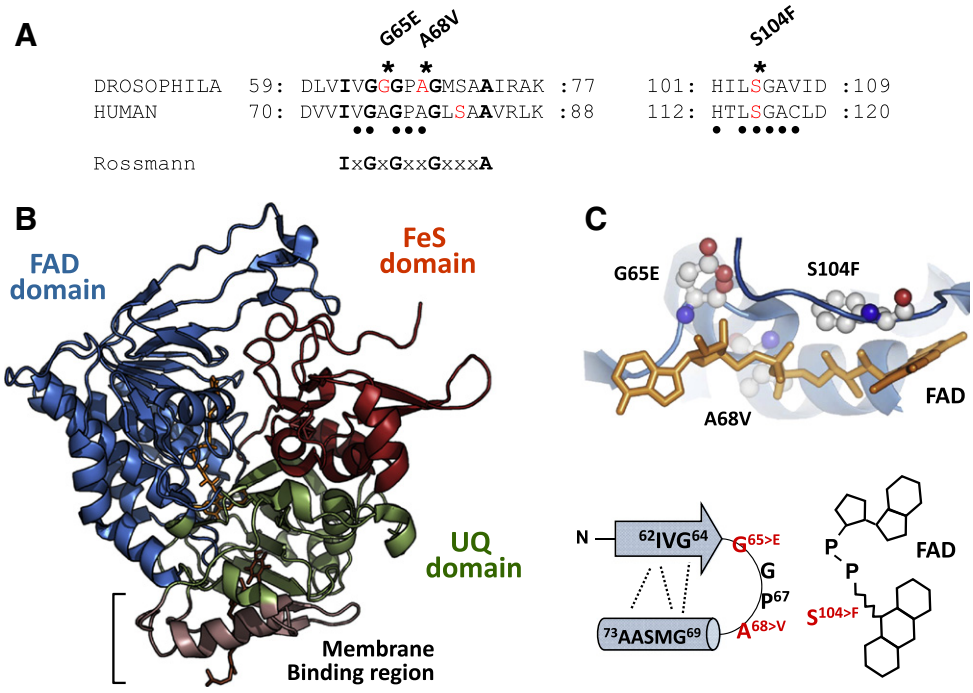

Fig. 4. Mutations map within the FAD binding residues and Rossmann fold. Panel A: Two of the identified mutations in fly *ETF:QO* alleles (marked with asterisk, top alignment) map at the Rossmann fold (G65E and A68V), more specifically at FAD interacting positions (marked with dots in the alignment) and are found at the connecting loop between the beta sheet and the alpha helix. The other mutation (S104F) also involves a position interacting with FAD at the level of the flavin C2 carbon. Panel B: ETF:QO cartoon depicting the different structural domains in the protein. Panel C: Structural detail of ETF:QO on which the identified mutations have been represented and a topological cartoon depicting the Rossmann fold and FAD. See Results and discussion for further details.

sequence determines cofactor interactions and stabilisation of the Rossmann fold itself.

Two of the three ETF:QO *Drosophila* mutations are precisely located in this connecting loop (Fig. S4). One of them affects position 65 in which a glycine is replaced by the negatively charged glutamate (G65E); this change is very deleterious for the protein as the inserted residue causes an electrostatic clash with the negative charges from the proximal pyrophosphate group from the FAD cofactor (Fig. S4D). Moreover, the corresponding residue in the experimentally determined ETF:QO porcine structure is an alanine, whose side chain methyl group is indeed buried in a hydrophobic pocket (Fig. S4A). Therefore, the replacement for a large hydrophilic residue, such as the one from the glutamate, is indeed expected to be detrimental (Fig S4D). The other mutation in the segment involves position 68, and in this case an alanine is replaced by a valine (A68V); the mutated alanine is hydrogen bonded to the FAD pyrophosphate group through the main chain amide nitrogen atom (Fig. S4B). Therefore the bulkier apolar side chain from a valine will perturb the protein fold at the FAD binding site, which is certainly resulting in an impaired interaction with the cofactor (Fig. S4E). Interestingly, a mutation in the same relative position has been found in one of the *C. elegans* ETF:QO mutant alleles. In the nematode, this position in the primary sequence of ETF:QO corresponds to a serine, a conservative change in respect to the alanine found in the human and *Drosophila* proteins (see Fig. 4A). The change to a phenylalanine reported in the allele *s2447* of *let-721* results in maternal effect lethality [16]. This finding corroborates the view that this is indeed a hotspot segment region as mutations in these two specific positions within the nucleotide binding motif of the Rossmann fold are anticipated to clearly affect FAD binding. The remaining mutation is found further in the sequence at position 104, no longer within the Rossmann fold, but still in a sequence stretch that harbours several residues that interact with the isoallozaxine ring system of the FAD cofactor (Fig. S4C and F). The affected residue in this case is a serine which is replaced by the bulkier aromatic phenylalanine (S104F). This particular serine is a key residue in FAD interaction as its side chain hydroxyl group is hydrogen bonded to that of the FAD C2 carbon (Fig. S4C). Therefore, the insertion of a phenylalanine and its large aromatic ring severely displaces this interaction, disrupting FAD binding and consequently protein folding (Fig. S4F). In fact, a mutation in this position in human ETF:QO completely abolishes soluble protein, thus confirming the key role of cofactors in the stability of the protein (Frank Frerman, personal communication). Overall, the structural analysis of the mutations identified in the *ETF:QO* mutant alleles provides a molecular rationale for the observed lethal phenotypes and anomalous metabolic profile, as they severely influence the FAD interaction affecting the protein structural integrity and biological function.

3.7. Drosophila as a potential working model for MADD

Fatty acid oxidation (FAO) is a key cellular process in mitochondrial metabolism as it affords a high supply of energy in tissues with elevated metabolic rates such as heart and skeletal muscles [37]. Impaired fatty acid oxidation as in MADD leads to the accumulation of metabolic intermediates, down regulation of oxidative phosphorylation and Warburg switching for energy production. The magnitude of mitochondrial dysfunction relates to the severity of the functional impairment of the pathway, which in turn relates to the affected gene and severity of the genetic lesion. Model organisms have proven to be valuable tools to address defective β-oxidation disorders [38–41], and MADD in particular [15,16]. To our knowledge other detailed available studies on *Drosophila* FAO proteins focus on *colt*, a gene implicated in early embryonic development which encodes for a carnitine acylcarnitine carrier (CACT) [42], and *Enigma*, a gene encoding for a homologue of the acyl-CoA dehydrogenase 9 (ACAD9) which upon mutation results in perturbed lipid homeostasis, resistance to oxidative stress and a longevity phenotype [43]. In humans, ACAD9 has a long-chain acyl-CoA dehydrogenase activity in embryos and in the foetal brain [44]. Some other studies also suggest that FAO is a key pathway in *Drosophila*, intertwined with

other processes: for example ETF:QO is up-regulated as a response to a 24 hour starvation [45] and as a result of mitochondrial dysfunction resulting from conditions mimicking mitochondrial disease [46].

Mining of the *Drosophila* genome shows the presence of homologues of the mammalian proteins involved in fatty acid oxidation and transport whose transcriptome analysis denotes important expression levels of these proteins at early stages of development (Table S2 and Fig. S1), suggesting that this organism could be useful to study FAO defects.

Drosophila can in fact be envisaged as a potential working model for MADD, as shown by the work here reported, as the three mutant alleles identified in the *ETF:QO* gene result in low protein levels and a lethal phenotype, as a result of point mutations at the ETF:QO FAD binding region. If identical mutations would be found in humans they would account for a severe form of the disease, with probable embryonic death (MADD type II). In such circumstances, the underlying molecular defects are not analysed as in such instances there is rarely evidence for a defect in β-oxidation, unless in the cases of neonatal death for which the so-called metabolic autopsy is carried out post-mortem [20,37,47,48].

4. Conclusions

Here we have addressed lethal mutations in ETF:QO which reproduce the biochemical defects observed in the severe forms of MADD in humans, thus establishing the proof of principle concerning the suitability of using *Drosophila* as a model for MADD. The studied alleles allowed correlating embryonic-stage morphogenetic and biochemical defects with a particular type of structural defect within the FAD binding region of the Rossmann fold that impaired flavin binding and correct protein folding. This type of analysis using model organisms is extremely powerful, for example by providing a testable platform to identify what would be the *in vivo* effects of mutations identified in less severe forms of the disease, in respect to affected pathways or mitochondrial dysfunction. For the mutations yielding mild clinical phenotypes, a fly model would provide the unique opportunity for studying how MADD affects the different stages of development, from the embryo stages to the adult fly. This system would not only contribute to a substantially better knowledge of the molecular processes' affect in MADD but would also, in the long run, contribute for the design and testing of potential drugs, from pharmacological chaperones [49] to metabolites or their analogues [5].

Acknowledgements

Frank Frerman (University of Colorado Denver, USA) is gratefully acknowledged for discussion of results and for communicating unpublished data. Rikke Olsen (Aarhus University, Denmark) is acknowledged for the kind gift of a ETF:QO antibody. Adriano Henriques and Mónica Serrano (ITQB) are greatly acknowledged for advice on molecular biology methods. This work was partly supported by the Fundação para a Ciência e Tecnologia (FCT/MCTES, Portugal) through: research grant PTDC/SAU-GMG/70033/2006 (to C.M.G), PTDC/QUI-BIQ/113027/2009, PTDC/BIA-BCM/111822/2009, and PTDC/SAU-BID/111796/2009 (to R.G.M.), fellowships SFRH/BPD/41609/2007 (to E.A.), SFRH/BPD/74475/2010 (to B.J.H.) and SFRH/BPD/34763/2007 (to J.V.R), and by the strategic grant PEst-OE/EQB/LA0004/2011 (to ITQB Laboratório Associado). This work was also partly supported by a CLIMB UK 'Children living with metabolic disease' research grant (to C.M.G.).

Appendix A. Supplementary data

Supplementary data to this article can be found online at http://dx.doi.org/10.1016/j.bbadis.2012.05.003.

References

[1] Z. Swigonova, A.W. Mohsen, J. Vockley, Acyl-CoA dehydrogenases: dynamic history of protein family evolution, J. Mol. Evol. 69 (2009) 176–193.
[2] B.J. Henriques, R.K. Olsen, P. Bross, C.M. Gomes, Emerging roles for riboflavin in functional rescue of mitochondrial beta-oxidation flavoenzymes, Curr. Med. Chem. 17 (2010) 3842–3854.
[3] B.J. Henriques, P. Bross, C.M. Gomes, Mutational hotspots in electron transfer flavoprotein underlie defective folding and function in multiple acyl-CoA dehydrogenase deficiency, Biochim. Biophys. Acta 1802 (2010) 1070–1077.
[4] B.J. Henriques, J.V. Rodrigues, R.K. Olsen, P. Bross, C.M. Gomes, Role of flavinylation in a mild variant of multiple acyl-CoA dehydrogenation deficiency: a molecular rationale for the effects of riboflavin supplementation, J. Biol. Chem. 284 (2009) 4222–4229.
[5] T.G. Lucas, B.J. Henriques, J.V. Rodrigues, P. Bross, N. Gregersen, C.M. Gomes, Co-factors and metabolites as potential stabilizers of mitochondrial acyl-CoA dehydrogenases, Biochim. Biophys. Acta 1812 (2011) 1658–1663.
[6] T.M. Dwyer, S. Mortl, K. Kemter, A. Bacher, A. Fauq, F.E. Frerman, The intraflavin hydrogen bond in human electron transfer flavoprotein modulates redox potentials and may participate in electron transfer, Biochemistry 38 (1999) 9735–9745.
[7] J.V. Rodrigues, C.M. Gomes, Mechanism of Superoxide and Hydrogen Peroxide Generation by Human Electron Transfer Flavoprotein and Pathological Variants, Free Radical Biology and Medicine (2012).
[8] D.L. Roberts, F.E. Frerman, J.J. Kim, Three-dimensional structure of human electron transfer flavoprotein to 2.1-A resolution, Proc. Natl. Acad. Sci. U. S. A. 93 (1996) 14355–14360.
[9] J. Zhang, F.E. Frerman, J.J. Kim, Structure of electron transfer flavoprotein–ubiquinone oxidoreductase and electron transfer to the mitochondrial ubiquinone pool, Proc. Natl. Acad. Sci. U. S. A. 103 (2006) 16212–16217.
[10] R.P. McAndrew, Y. Wang, A.W. Mohsen, M. He, J. Vockley, J.J. Kim, Structural basis for substrate fatty acyl chain specificity: crystal structure of human very-long-chain acyl-CoA dehydrogenase, J. Biol. Chem. 283 (2008) 9435–9443.
[11] H.J. Lee, M. Wang, R. Paschke, A. Nandy, S. Ghisla, J.J. Kim, Crystal structures of the wild type and the Glu376Gly/Thr255Glu mutant of human medium-chain acyl-CoA dehydrogenase: influence of the location of the catalytic base on substrate specificity, Biochemistry 35 (1996) 12412–12420.
[12] J.J. Kim, M. Wang, R. Paschke, Crystal structures of medium-chain acyl-CoA dehydrogenase from pig liver mitochondria with and without substrate, Proc. Natl. Acad. Sci. U. S. A. 90 (1993) 7523–7527.
[13] K.P. Battaile, J. Molin-Case, R. Paschke, M. Wang, D. Bennett, J. Vockley, J.J. Kim, Crystal structure of rat short chain acyl-CoA dehydrogenase complexed with acetoacetyl-CoA: comparison with other acyl-CoA dehydrogenases, J. Biol. Chem. 277 (2002) 12200–12207.
[14] G. Kleiger, D. Eisenberg, GXXXG and GXXXA motifs stabilize FAD and NAD(P)-binding Rossmann folds through C(alpha)–H. O hydrogen bonds and van der waals interactions, J. Mol. Biol. 323 (2002) 69–76.
[15] Y. Song, M.A. Selak, C.T. Watson, C. Coutts, P.C. Scherer, J.A. Panzer, S. Gibbs, M.O. Scott, G. Willer, R.G. Gregg, D.W. Ali, M.J. Bennett, R.J. Balice-Gordon, Mechanisms underlying metabolic and neural defects in zebrafish and human multiple acyl-CoA dehydrogenase deficiency (MADD), PLoS One 4 (2009) e8329.
[16] D.S. Chew, A.K. Mah, D.L. Baillie, Characterizing the transcriptional regulation of let-721, a *Caenorhabditis elegans* homolog of human electron flavoprotein dehydrogenase, Mol. Genet. Genomics 282 (2009) 555–570.
[17] A. Pimenta-Marques, R. Tostoes, T. Marty, V. Barbosa, R. Lehmann, R.G. Martinho, Differential requirements of a mitotic acetyltransferase in somatic and germ line cells, Dev. Biol. 323 (2008) 197–206.
[18] T.B. Chou, N. Perrimon, Use of a yeast site-specific recombinase to produce female germline chimeras in Drosophila, Genetics 131 (1992) 643–653.
[19] L.G. Guilgur, P. Prudencio, T. Ferreira, A.R. Pimenta-Marques, R.G. Martinho, Drosophila aPKC is required for mitotic spindle orientation during symmetric division of epithelial cells, Development 139 (2012) 503–513.
[20] M.S. Rashed, P.T. Ozand, M.P. Bucknall, D. Little, Diagnosis of inborn errors of metabolism from blood spots by acylcarnitines and amino acids profiling using automated electrospray tandem mass spectrometry, Pediatr. Res. 38 (1995) 324–331.
[21] C. Watters, A one-step Biuret assay for protein in the presence of detergent, Anal. Biochem. 88 (1978) 695–698.
[22] C. Welinder, L. Ekblad, Coomassie staining as loading control in Western blot analysis, J. Proteome Res. 10 (2011) 1416–1419.
[23] R.K. Olsen, B.S. Andresen, E. Christensen, P. Bross, F. Skovby, N. Gregersen, Clear relationship between ETF/ETFDH genotype and phenotype in patients with multiple acyl-CoA dehydrogenation deficiency, Hum. Mutat. 22 (2003) 12–23.
[24] J.D. Beckmann, F.E. Frerman, Electron-transfer flavoprotein–ubiquinone oxidoreductase from pig liver: purification and molecular, redox, and catalytic properties, Biochemistry 24 (1985) 3913–3921.
[25] J.D. Beckmann, F.E. Frerman, Reaction of electron-transfer flavoprotein with electron-transfer flavoprotein–ubiquinone oxidoreductase, Biochemistry 24 (1985) 3922–3925.
[26] K.B. Nicholas, H.B. Nicholas, D.W. Deerfield, GeneDoc: analysis and visualization of genetic variation, EMBNEW NEWS 4 (1) (1997) 1–4.
[27] G. Vriend, WHAT IF: a molecular modeling and drug design program, J. Mol. Graph. 8 (1990) 52–56 (29).
[28] M.C. McKean, J.D. Beckmann, F.E. Frerman, Subunit structure of electron transfer flavoprotein, J. Biol. Chem. 258 (1983) 1866–1870.
[29] W. Rhead, V. Roettger, T. Marshall, B. Amendt, Multiple acyl-coenzyme A dehydrogenation disorder responsive to riboflavin: substrate oxidation, flavin metabolism, and flavoenzyme activities in fibroblasts, Pediatr. Res. 33 (1993) 129–135.

[30] F.W. Studier, Protein production by auto-induction in high density shaking cultures, Protein Expr. Purif. 41 (2005) 207–234.
[31] X. Liu, I. Kiss, J.A. Lengyel, Identification of genes controlling malpighian tubule and other epithelial morphogenesis in *Drosophila melanogaster*, Genetics 151 (1999) 685–695.
[32] W. Lehnert, U. Wendel, S. Lindenmaier, N. Bohm, Multiple acyl-CoA dehydrogenation deficiency (glutaric aciduria type II), congenital polycystic kidneys, and symmetric warty dysplasia of the cerebral cortex in two brothers. I. Clinical, metabolical, and biochemical findings, Eur. J. Pediatr. 139 (1982) 56–59.
[33] F.E. Frerman, S.I. Goodman, Deficiency of electron transfer flavoprotein or electron transfer flavoprotein:ubiquinone oxidoreductase in glutaric acidemia type II fibroblasts, Proc. Natl. Acad. Sci. U. S. A. 82 (1985) 4517–4520.
[34] A.D. Colevas, J.L. Edwards, R.H. Hruban, G.A. Mitchell, D. Valle, G.M. Hutchins, Glutaric acidemia type II. Comparison of pathologic features in two infants, Arch. Pathol. Lab. Med. 112 (1988) 1133–1139.
[35] G.N. Wilson, J.P. de Chadarevian, P. Kaplan, J.P. Loehr, F.E. Frerman, S.I. Goodman, Glutaric aciduria type II: review of the phenotype and report of an unusual glomerulopathy, Am. J. Med. Genet. 32 (1989) 395–401.
[36] M. Simkovic, G.D. Degala, S.S. Eaton, F.E. Frerman, Expression of human electron transfer flavoprotein–ubiquinone oxidoreductase from a baculovirus vector: kinetic and spectral characterization of the human protein, Biochem. J. 364 (2002) 659–667.
[37] M.J. Bennett, P. Rinaldo, A.W. Strauss, Inborn errors of mitochondrial fatty acid oxidation, Crit. Rev. Clin. Lab. Sci. 37 (2000) 1–44.
[38] R.J. Tolwani, D.A. Hamm, L. Tian, J.D. Sharer, J. Vockley, P. Rinaldo, D. Matern, T.R. Schoeb, P.A. Wood, Medium-chain acyl-CoA dehydrogenase deficiency in gene-targeted mice, PLoS Genet. 1 (2005) e23.
[39] H. Skilling, P.M. Coen, L. Fairfull, R.E. Ferrell, B.H. Goodpaster, J. Vockley, E.S. Goetzman, Brown adipose tissue function in short-chain acyl-CoA dehydrogenase deficient mice, Biochem. Biophys. Res. Commun. 400 (2010) 318–322.
[40] A.A. Werdich, F. Baudenbacher, I. Dzhura, L.H. Jeyakumar, P.J. Kannankeril, S. Fleischer, A. LeGrone, D. Milatovic, M. Aschner, A.W. Strauss, M.E. Anderson, V.J. Exil, Polymorphic ventricular tachycardia and abnormal Ca2+ handling in very-long-chain acyl-CoA dehydrogenase null mice, Am. J. Physiol. Heart Circ. Physiol. 292 (2007) H2202–H2211.
[41] M. Chegary, H. Brinke, J.P. Ruiter, F.A. Wijburg, M.S. Stoll, P.E. Minkler, M. van Weeghel, H. Schulz, C.L. Hoppel, R.J. Wanders, S.M. Houten, Mitochondrial long chain fatty acid beta-oxidation in man and mouse, Biochim. Biophys. Acta 1791 (2009) 806–815.
[42] N.A. Oey, L. Ijlst, C.W. van Roermund, F.A. Wijburg, R.J. Wanders, dif-1 and colt, both implicated in early embryonic development, encode carnitine acylcarnitine translocase, Mol. Genet. Metab. 85 (2005) 121–124.
[43] P. Mourikis, G.D. Hurlbut, S. Artavanis-Tsakonas, Enigma, a mitochondrial protein affecting lifespan and oxidative stress response in *Drosophila*, Proc. Natl. Acad. Sci. U. S. A. 103 (2006) 1307–1312.
[44] N.A. Oey, J.P. Ruiter, T. Attie-Bitach, L. Ijlst, R.J. Wanders, F.A. Wijburg, Fatty acid oxidation in the human fetus: implications for fetal and adult disease, J. Inherit. Metab. Dis. 29 (2006) 71–75.
[45] K. Fujikawa, A. Takahashi, A. Nishimura, M. Itoh, T. Takano-Shimizu, M. Ozaki, Characteristics of genes up-regulated and down-regulated after 24 h starvation in the head of *Drosophila*, Gene 446 (2009) 11–17.
[46] D.J. Fernandez-Ayala, S. Chen, E. Kemppainen, K.M. O'Dell, H.T. Jacobs, Gene expression in a *Drosophila* model of mitochondrial disease, PLoS One 5 (2010) e8549.
[47] M.S. Rashed, P.T. Ozand, M.J. Bennett, J.J. Barnard, D.R. Govindaraju, P. Rinaldo, Inborn errors of metabolism diagnosed in sudden death cases by acylcarnitine analysis of postmortem bile, Clin. Chem. 41 (1995) 1109–1114.
[48] T. Yamamoto, H. Tanaka, H. Kobayashi, K. Okamura, T. Tanaka, Y. Emoto, K. Sugimoto, M. Nakatome, N. Sakai, H. Kuroki, S. Yamaguchi, R. Matoba, Retrospective review of Japanese sudden unexpected death in infancy: the importance of metabolic autopsy and expanded newborn screening, Mol. Genet. Metab. 102 (2011) 399–406.
[49] P. Leandro, C.M. Gomes, Protein misfolding in conformational disorders: rescue of folding defects and chemical chaperoning, Mini Rev. Med. Chem. 8 (2008) 901–911.